

MULTIFUNCTIONAL BORON NITRIDE NANOTUBE (BNNT) COMPOSITES FOR EXTREME AEROSPACE ENVIRONMENTS

Alexander Hatfield¹, Dr. Tian-Bing Xu¹, Dr. Cheol Park², Dr. Sang-Hyon Chu²

¹ Old Dominion University, Department of Mechanical and Aerospace Engineering, Norfolk, VA 23529

² NASA Langley Research Center, Advanced Materials and Processing Branch, Hampton, VA 23681

Abstract

Boron Nitride Nanotubes (BNNTs) are a promising nanomaterial that can be utilized in various matrices to increase capabilities in thermal stability, mechanical strength, piezoelectric properties, and radiation shielding. By integrating these nanomaterials into various polymers, polyimide, and other matrices an investigation into the improvement of material properties can be made. Space and aeronautics applications have an ever-growing demand for enhanced materials, capable of performing tasks in extreme environments. The goal of this work is to address this need and provide a viable alternative to current industry practices. Performing the analysis of fabrication techniques, dispersion methods, and interaction with the mixing media we aim to achieve a uniform BNNT composite, more capable than its pristine counterpart. Through investigation of the fabrication techniques for uniformity, scalability, and ease of production, the most effective process to achieve rapid development of BNNT composites can be selected. This study will highlight the material improvements based on the nanofiller content and provide an alternative material option for harsh environment operations in a variety of fields.

Introduction

Space exploration and aerospace applications have a constant need for material improvements. Their harsh environments demand materials that can

withstand the large temperature ranges, mechanical stresses, and other requirements such as radiation shielding or corrosion resistance [1-3]. Being able to operate in temperatures ranging from cryogenic conditions to upwards of 500 °C is a staple of these industries, and reducing weight of the materials that can achieve operation in these conditions is key [2]. Space applications have exposure to ionizing radiation stemming from galactic cosmic radiation (GCR), particles from solar flares, and other solar events that can deteriorate materials and endanger human life [4]. Mechanically robust, thermally and chemically stable, and electrically enhanced, transparent composites are needed to advance space travel and safe human operation for a permanent presence on extraterrestrial surfaces such as the Moon.

Understanding these needs enables the problem to be addressed through the introduction of alternative material solutions, including boron nitride nanotube (BNNT) composites. These nanomaterials provide essential material properties and can be used as a filler to improve the performance of base polymers, e.g., polyimides and polyvinylidene fluoride (PVDF), in multiple ways. BNNTs exhibit great neutron absorption due to the boron content, are thermally stable in air up to 800 °C, and have high tensile strength up to 50 GPa. BNNTs also provide high thermal

conductivity up to 600 W/m·K, piezoelectric capabilities, and a wide bandgap of 5.5 eV [5-11]. Compared to carbon nanotubes (CNTs), BNNTs exhibit better electrical insulation, chemical and thermal stability, and piezoelectricity while maintaining equal or similar thermal conductivity and mechanical robustness [12,13].

To facilitate BNNT incorporation, multiple polymer composites were fabricated and characterized, namely, colorless polyimide 1 and 2 (LaRC™-CP1 and LaRC™-CP2) and polyvinylidene fluoride (PVDF) owing to their transparent nature and advantageous material properties. The nanofiller itself also has a variety of forms that were assessed to parametrically disperse into these base matrices, such as BNNS (Boron Nitride Nanosheets or hBN) and BNNT “puffballs” (a typical form of BNNTs), as seen in Figure 1. Each of these forms has advantages and disadvantages that will be discussed.

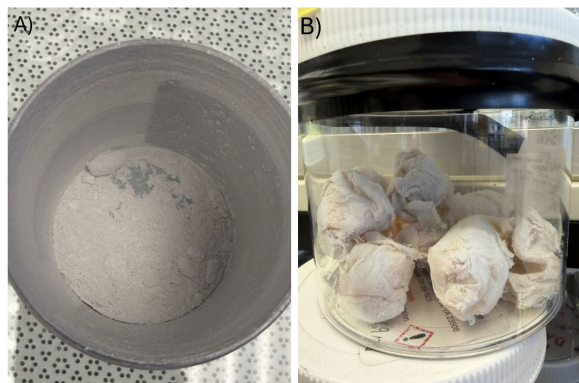


Figure 1: Different forms of BN Nanomaterial: A) BNNS or hBN powder, B) BNNT puffball

Fabrication Techniques and Methodology

Proper dispersion of nanofiller material is key to the success of an enhanced composite and its resulting material properties. In some cases, poor dispersion can even lead to worse material performance

compared to a composite with a lower loading level. The methods that were explored over tens to hundreds of composite film fabrication were the following: cup horn sonication, sonication bath, homogenization, acoustic mixing, speed mixing, and in-situ polymerization with a nitrogen purge as seen in Figure 2. Various combinations of the mentioned methods were attempted, and clear indications of proper dispersion were found. Dispersion properties are dependent on multiple factors that can make even an “optimal” setup ineffective, including human error and environmental conditions such as humidity, but for the most part an optimal experimental design was identified.



Figure 2: Various equipment used for dispersion experiments: A) bath sonicator, B) three-neck flask setup for in-situ polymerization, C) cup horn sonicator, D) acoustic mixer

The configuration for fabrication of the nanofiller composition followed the same protocol across samples, only deviating for investigations into the effects

of variable changes for different forms of BNNTs. Dispersion of the BNNT is first achieved by preparing a slurry consisting of the targeted weight percentage (wt.%) using appropriate amounts of the solvent, dimethylacetamide (DMAc). This process consists of acoustic mixing, cup horn sonication, and a bath sonication, with the order being dependent on the type of nanotube. For example, for the puffballs, we start with acoustic mixing to unravel and separate the strands into a more easily dispersible micro-level slurry. After acoustic mixing the slurry would then be cup horn sonicated, followed by being combined with the polymer material and lastly placed in a sonication bath with mechanical mixing the solution in a three-neck flask. Identifying proper dispersion methods for bulk material and attributing proper dispersion to increased material properties was a key part of this research.

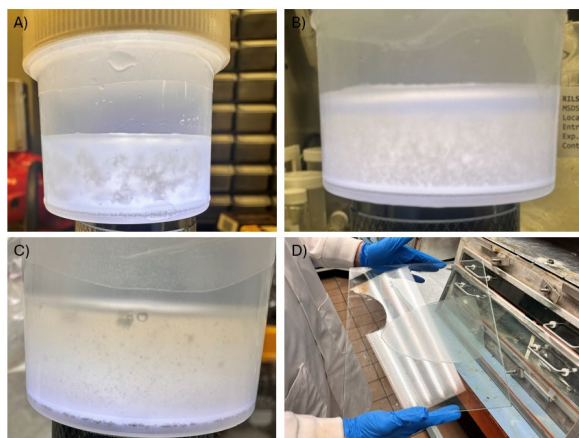


Figure 3: Process of dispersion: A) BNNT after cup horn sonication, B) BNNT after acoustic mixing, C) BNNT and polymer (CP1) after sonication bath and in-situ polymerization setup, D) solution cast onto glass plate to make a thin film

After the mixing and dispersion of the nanomaterial into a solution containing the polymer matrix, seen in Figure 3, the samples were then cast onto a glass plate via a doctor's blade with a thickness set by a

filler gauge and placed into a dry box for over twenty-four hours (time dependent on thickness and solvent composition) until the sample solidifies. Once the film is properly dried it is then placed into an oven with a nitrogen purge to bake out all solvents and cure the polymer base. The bake out procedure depends on the polymer base, but the final target temperature is normally right above T_g (glass transition temperature) of the polymer.

Characterization and Testing

Testing of these thin films consisted of mechanical testing, thermal testing, and electrical testing. Consistent data for most of these tests were hard to collect due to the changing levels of dispersion from manufacturing techniques. For this discussion, only a few tests will be highlighted, specifically the ferroelectric testing process, seen in Figure 4. Other characterization techniques that will be discussed are optical microscopy and scanning electron microscopy (SEM) imaging, used to visually evaluate dispersion levels and correlate the observation with material properties.



Figure 4: A) Ferroelectric testing equipment, B) optical microscope, and C) SEM testing equipment

The preparation for these testing methods depended on the specific characterization. For SEM imaging, for

example, the samples had to be immersed in liquid nitrogen (LN₂) until becoming brittle, then were snapped with a pair of tweezers to get a cross-sectional fracture surface for SEM analysis. Once snapped, the samples received a light coating of gold-palladium via sputtering and then imaged accordingly at various magnifications, seen in Figure 5.

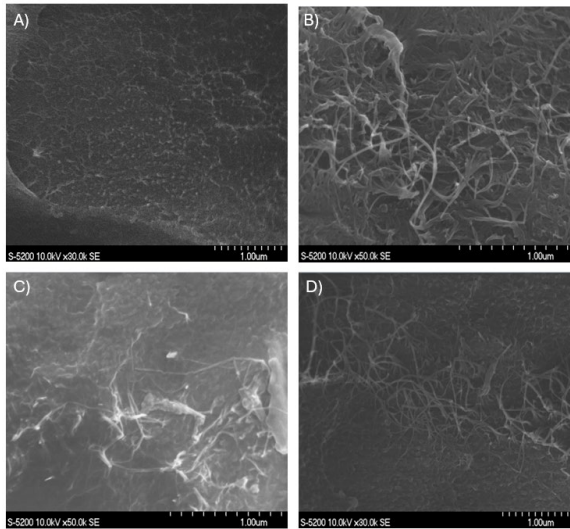


Figure 5: Comparison of PVDF composites A) Pristine PVDF, B) 0.5 wt.% BNNT PVDF, C) 0.5 wt.% BNNT PVDF (different mixing parameters), D) 1 wt.% BNNT PVDF

Optical microscopy of the samples was done by swapping out the stage and lighting for a transmitted lighting setup to be able to see nanofiller materials and address the dispersion quality of the composite. Ferroelectric samples were prepared by cutting out representative 1” (25.4 mm) rounds and “shadow masking” them to account for the edge capacitance effect, ensuring the gold coatings do not reach the outer edges of the sample to avoid arcing and shorting during testing. Once the samples are cut out and masked, they are coated via thermal evaporation with a base layer of 15 nm of chromium, followed by 135 nm of gold, with thickness monitored by a quartz crystal thickness sensor inside the

thermal evaporator chamber. Alternatively, a magnetron sputtering device was used with a purely gold coating around 150 nm thickness for some samples. Once coated properly to create a parallel plate out of the sample, they are then put into the ferroelectric setup and submerged in silicon oil to assist with the dielectric breakdown of air (2 MV/m) and avoid sample damage when reaching higher levels of voltage.

Results and Discussion

The primary focus of this work was to increase the piezoelectricity of transparent materials by including nanofillers. As seen in Figure 6, commercial ceramics have been used as a baseline and reference due to their great piezoelectric properties, but they lack transparency and flexibility which a lot of aerospace processes desire.

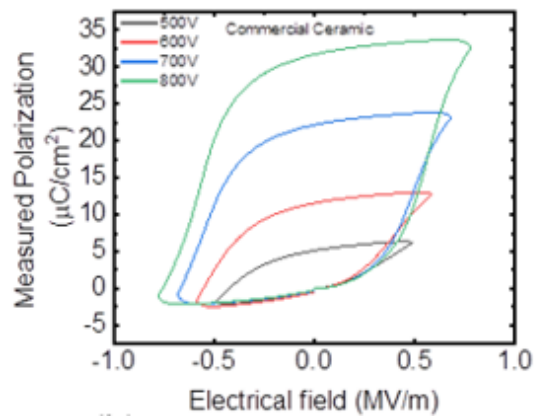


Figure 6: Commercial PZT reference hysteresis loop

Due to the inherent ability of PVDF polymers to possess dipoles and piezoelectricity it was chosen as a good starting point for composite manufacturing and electrical testing with nanofiller content. To get an unbiased base line, all PVDF samples were manufactured in the same manner without post processing, meaning no stretching or alignment of dipoles via

polling process, except for the 0.5 wt.% samples that had two different processing parameters to be used as a comparison. For reference, 0.5 wt.% acoustic mixed (AM) and 0.5 wt.% speed mixed (SM) refer to the process being used. The nanofiller used for these samples is the BNNT puffball variety. By performing a hysteresis loop and applying voltage to the samples the response can be monitored and recorded for piezoelectric effects, seen in Figure 7.

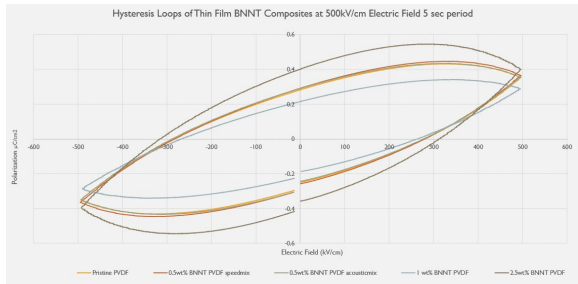


Figure 7: Pristine to 2.5 wt.% BNNT puffball hysteresis comparative loop to 5 MV/m

As seen in Figure 8, the remanent polarization tends to increase with increasing BNNT concentration except for 1 wt.% case. Looking at this data in Figures 7 and 8, we have an outlier in the 1 wt.% BNNT PVDF film, and the 0.5 wt.% inclusions increase the remnant polarization of the pristine material. The 2.5 wt.% BNNT PVDF film, however, has a clear increase in its inherent piezoelectric properties.

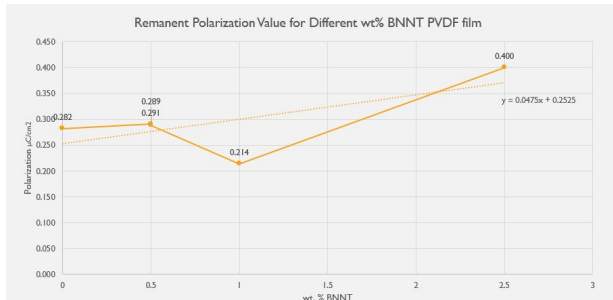


Figure 8: Comparison of the remanent polarization for each sample from 0–2.5 wt.% BNNT nanofiller

To understand this anomaly for 1 wt.% sample in data and trend an extensive optical microscopy analysis was performed for each sample to ascertain the quality of dispersion and determine if poor dispersion might be a factor in the observed deviation. It was found that dispersion clearly plays a key role in the material properties and enhances piezoelectric performance. As seen in Figure 9, a direct comparison of the 1 wt.% sample and 2.5 wt.% sample shows that, even with increased amounts of nanofiller, the 2.5 wt.% sample has much less visible agglomerations of material and is generally better dispersed than the 1 wt.% sample.

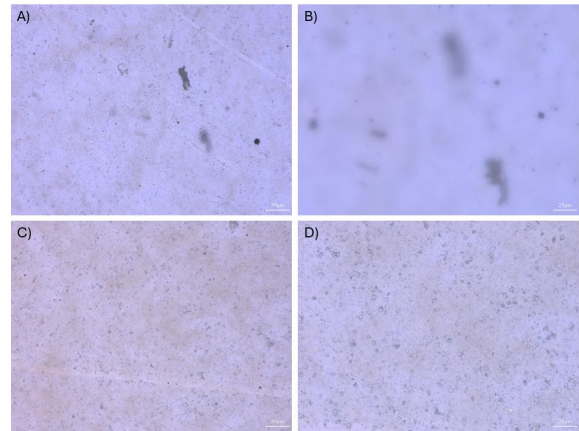


Figure 9: Depth composition (Z-stitched images) for 1 wt.% and 2.5 wt.% BNNT PVDF samples. A) 500x 1 wt.%, B) 1000x 1 wt.%, C) 500x 2.5 wt.%, D) 1000x 2.5 wt.%

In addition, as seen in Figure 9, the agglomerations dominate in the 1 wt.% sample. Under depth-composition imaging, the optical microscope was unable to maintain focal clarity beyond the agglomerate due to the large height discontinuity, whereas the 2.5 wt.% sample exhibited uniform topography that allowed the entire field to remain in focus. For a better understanding, Figure 10 shows a “static” image taken at a single focal depth for the same sample setup.

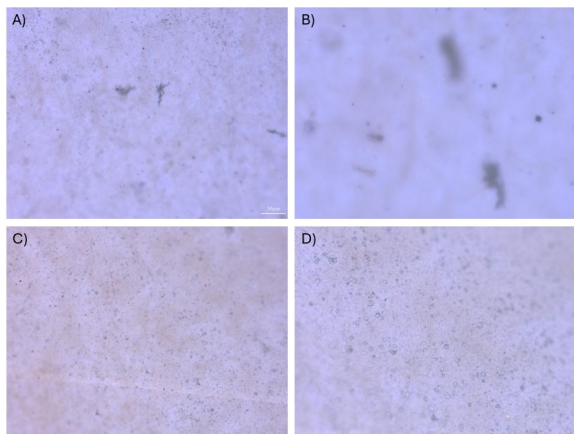


Figure 10: Static imaging A) 500x 1 wt.%, B) 1000x 1 wt.%, C) 500x 2.5 wt.%, D) 1000x 2.5 wt.%

To help further explain this depth composition Figures 11 and 12 show the process involved in creating one of these Z-stitched images.

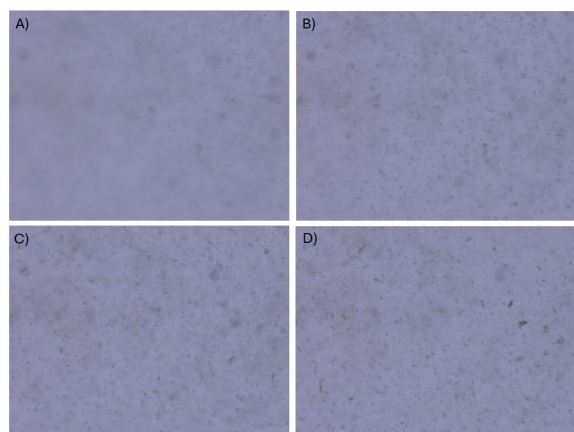


Figure 11: 1 μm per layer distance at 1000x magnification of a 1 wt.% BNNT+BNNS CP1 composite A) bottom layer, B) 5 layers up, C) 10 layers up, D) 15 layers up

Essentially the software and microscope work together to take multiple images of the same sample over the thickness of the sample at a set pitch, in the case of Figures 11 and 12 this pitch is 1 image per 1 micron moved in the z-axis. This allows us to see through thickness dispersion and allow for total focus of the samples thickness seen by transmitted light.

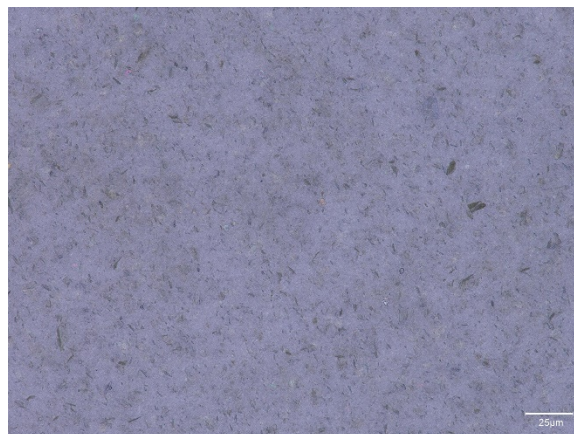


Figure 12: 1000x depth composition image, stitched together 25 layers, 1 wt.% BNNT+BNNS CP1 composite

Conclusions

Dispersion is a critical factor in the development of enhanced polymer composites. While further investigation is required to draw conclusions about the effects of incorporating these nanomaterials into the polymers to increase their inherent properties, as proof of concept, we have further optimized dispersion of nanomaterials in polymer matrices and have observed improvement in material performance. Future work should include making a material set under the same processing conditions and ensuring similar dispersion is seen throughout the sample set. Once that is well established for various polymer matrices, material property testing should conclude in consistent, repeatable testing and results.

Acknowledgements

Special thanks to NASA LaRC Interns Jenny Campbell for her help with the dispersion of nanomaterials, Peter Le for his assistance with SEM imaging, and Wade Collins for his assistance with ferroelectric testing. Without them we would not have had enough time to investigate as many items as we did. Thank you to my advisor Dr. Tian-

Bing Xu for providing me with the opportunity to interface and work with all the wonderful people I have met at NASA. And lastly, thank you to Dr. Cheol Park and Dr. Sang-Hyon Chu for their assistance, training, and mentorship. Thank you as well to the Virginia Space Grant Consortium and NASA RSAA210713 program for supporting me throughout my time as a graduate student.

References

- [1] Bhat, B. N. (n.d.). Materials challenges in space exploration. National Aeronautics and Space Administration, George C. Marshall Space Flight Center. <https://ntrs.nasa.gov/api/citations/20050092366/downloads/20050092366.pdf>
- [2] Bond, D. K., Goddard, B., Singleterry, R. C., & Bilbao y León, S. (2020). Comparing the Effectiveness of Polymer and Composite Materials to Aluminum for Extended Deep Space Travel. *Nuclear Technology*, 206(8), 1120–1139. <https://doi.org/10.1080/00295450.2019.1681221>
- [3] Wani, I. N., Aggarwal, K., Bishnoi, S., Shukla, P. K., Harursamath, D., & Garg, A. (2025). Materials used in space shuttle: Evolution, challenges, and future prospects—An overview. *Composites Part B: Engineering*, 303, 112540. <https://doi.org/10.1016/j.compositesb.2025.112540>
- [4] Durante, M., & Cucinotta, F. A. (2011). Physical basis of radiation protection in space travel. *Reviews of Modern Physics*, 83, 1245. <https://doi.org/10.1103/RevModPhys.83.1245>
- [5] Kostoglou, N., Tampaxis, C., Charalambopoulou, G., Constantinides, G., Ryzhkov, V., Dومانidis, C., Matovic, B., Mitterer, C., & Rebholz, C. (2020). Boron

nitride nanotubes versus carbon nanotubes: A thermal stability and oxidation behavior study. *Nanomaterials*, 10(12), 2435.

<https://doi.org/10.3390/nano10122435>

[6] Chopra, N. G., et al. "Boron nitride nanotubes." *Science* 269.5226 (1995): 966-967 [10.1126/science.269.5226.966](https://doi.org/10.1126/science.269.5226.966)

[7] Lee, C.H., Bhandari, S., Tiwari, B., Yapici, N., Zhang, D., Yap, Y.K. Boron Nitride Nanotubes: Recent Advances in Their Synthesis, Functionalization, and Applications. *Molecules* 2016, 21, 922. <https://doi.org/10.3390/molecules2107092>

[8] Chen, X., Dmuchowski, C.M., Park, C. et al. Quantitative Characterization of Structural and Mechanical Properties of Boron Nitride Nanotubes in High Temperature Environments. *Sci Rep* 7, 11388 (2017). <https://doi.org/10.1038/s41598-017-11795-9>

[9] Snapp, P, Cho, C, Lee, D, Haque, M, Nam, S, Park, C, Tunable Piezoelectricity of Multifunctional Boron Nitride Nanotube/Poly(dimethylsiloxane) Stretchable Composites. *Adv. Mater.*2020, 32, 2004607. <https://doi.org/10.1002/adma.202004607>

[10] Park, C. (2014, March 10). Boron nitride nanotube: Synthesis and applications [Presentation slides]. *Macromolecular Science and Engineering*, University of Michigan, Ann Arbor, MI. <https://ntrs.nasa.gov/api/citations/20200007559/downloads/20200007559.pdf>

[11] Park, C., Chu, S.-H., & Fay, C. (n.d.). Boron nitride nanotube (BNNT) and BNNT composites: Overview [Presentation slides]. NASA Langley Research Center. <https://ntrs.nasa.gov/citations/20200003735>

[12] Kostoglou N, Tampaxis C, Charalambopoulou G, Constantinides G,

Ryzhkov V, Doumanidis C, Matovic B, Mitterer C, Rebholz C. Boron Nitride Nanotubes Versus Carbon Nanotubes: A Thermal Stability and Oxidation Behavior Study. *Nanomaterials* (Basel). 2020 Dec 5;10(12):2435. doi: [10.3390/nano10122435](https://doi.org/10.3390/nano10122435) PMID: 33291505; PMCID: PMC7762177.

[13] Cha, J., Jin, S., Shim, J. H., Park, C. S., Ryu, H. J., & Hong, S. H. (2016). Functionalization of carbon nanotubes for fabrication of CNT/epoxy nanocomposites. *Materials & Design*, 95, 1–8. <https://doi.org/10.1016/j.matdes.2016.01.077>